

# MULTIPLE ELEMENT INTERFEROMETER FOR LOCATING SOURCES OF SOLAR NOISE AT 4,000 MEGACYCLES (2)

HARUO TANAKA AND TAKAKIYO KAKINUMA

*Summary* — An 8-element interferometer with quarter-wavelength plates was completed in June, 1954. Each aerial has a paraboloidal reflector, 1.5 metre in diameter which can automatically follow the sun. Aerials are placed in E-W direction at 6.45 metres (86 $\lambda$ ) intervals. The main lobes are spaced 40' apart and have half-power widths of 4.5' around the local noon. Observations can be made for about five hours a day. Two dimensional location of radio spots is partially possible because the scanning direction gradually changes in a day except for the periods around the equinoxes. Quarter-wavelength plates are mounted over the paraboloidal reflectors and they can be driven simultaneously. They are so designed as to minimize the reflection. To improve the accuracy of measurement, a square-law detector is used and a hot load is prepared for daily calibrations.

## I. Introduction

A 5-element interferometer<sup>1)</sup> which had been in operation from March, 1953 to April, 1954 was dis-assembled and an 8-element interferometer with quarterwavelength plates was constructed in June, 1954.

The half-power width of each fan-shaped lobe is 4.5' in E-W direction, spaced 40' apart around the local noon. The lobe spacing may seem to be a little too narrow as compared with the radio diameter of the sun which is about 1.2 times that of the optical disk. It was selected so as to attain the highest possible resolving power with a given number of aerial elements as small as eight, because the wider lobe spacings in the direction far apart from the meridian plane are available if desired. The lobe is spaced about 49' at 35° away from the meridian plane.

It is remarkable that the location of a strongly enhanced region in two dimensional sense is possible except for the periods around the equinoxes. The scanning direction changes as much as 35 degrees in a day during the period around the solstice. A radio spot located in such a way agreed precisely with that determined by the solar eclipse on June 20, 1955 (see another paper in these Proceedings).

Now that the sun is substantially quiet, the deduction of the radio brightness distribution on the sun is the chief interest of our present research. As the solar activity increases, however, the location of radio spots as well as the determination of their size, intensity and polarization will become the main object of observations the results of which will be useful not only for research on the solar atmosphere but also for the warning of radio disturbances.

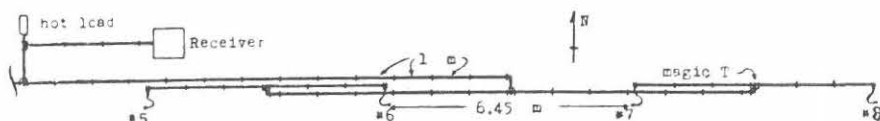
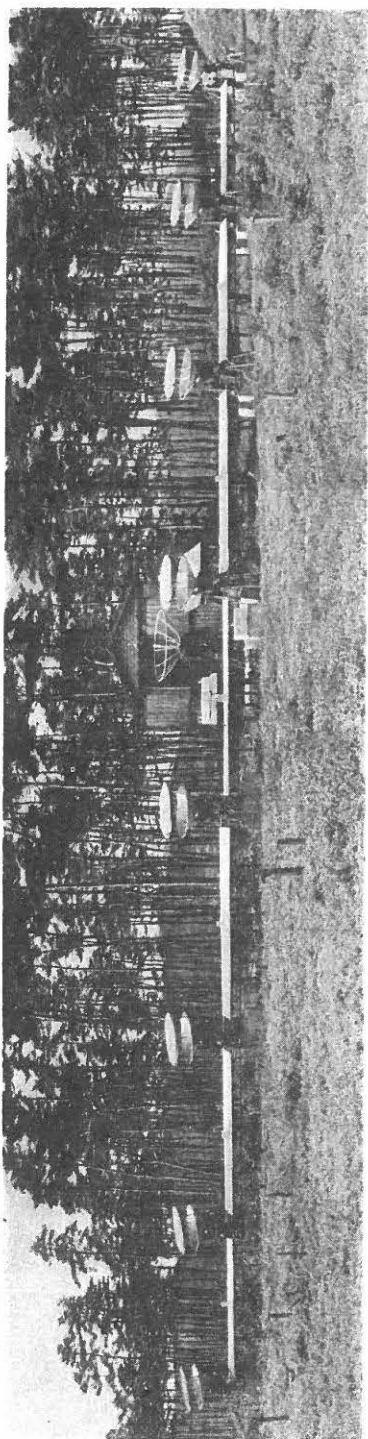


Fig. 1. The arrangement of transmission lines.



## II. Aerial system

We have already described in the last Proceedings<sup>1)</sup> some essential matters such as unit aerial, method of combining input signals, configuration of transmission lines, etc. and now it may be sufficient to explain additional features.

The arrangement of transmission lines is shown in Fig. 1. A switch is placed just ahead of a hot load which is ready for daily calibrations. A considerable length of feeder is inserted between the switch and the receiver for reducing errors due to the "substitution"<sup>2)</sup>. Aerial units are placed accurately in E-W direction and the height of each aerial was adjusted by means of a water level. As a result, the records obtained when the sun is quiet are quite symmetrical about the local noon.

As we pointed out in the last Proceedings<sup>1)</sup>, the spectral dispersion in the direction far apart from the meridian plane has no serious effect on the shape of directive patterns (see Fig. 12 on page 93).

## II. Equivalent noise temperature and transmission losses

The following measurements were made when the sun was quiet; the atmospheric temperature at the time was 303 °K. The background noise at the switch, placed ahead of the hot load, was 130° K in equivalent temperature, which was measured by directing all the aerials toward the empty sky. On the other hand, when they were directed toward the sun, the input noise increased by 211° K at the centre of the No. 0 drift curve.

Now, when the input signal of one aerial was separately led to the receiver using switches at magic tees<sup>1)</sup>, the noise signal increased by 157° K. Consequently the maximum signal of the complete aerial system should have been 1265 °K, eight times of 157°K, but it was only 211 °K by the above measurement. This contradiction arises from the fact that only a fraction of total radiation from the sun is received owing to the sharpness of directivity. The rate of decrease is clearly  $211/1256=0.168$ . This figure can also be obtained with good coincidence from calculations using a drift curve. Hence, if there is 10 percent enhanced radiation due to a small radio spot on the solar disk, the record of our interfero-

meter will have a peak 60 percent as high as the centre of the quiet level,

Transmission losses were measured indirectly from a series of experiments as follows: —

(1) We connected a large horn, 2 metres in length, to the input waveguide near the hot load and directed it toward the zenith as shown in Fig. 2 (1). The equivalent temperature of the input was 3°K.

(2) We connected then the same horn to the end of the waveguide under one of the unit aerials. All magic tees lying in its way were changed into bends so that only the signal in question can arrive at the receiver (see Fig. 2 (2)). The result was 84°K.

(3) Under the same conditions we obtained 117°K when we connected the horn to the upper end of the cable as shown in Fig. 2(3).

(4) Returning the cable to its ordinary place, we obtained 130°K (see Fig. 2(4)). Here, the relation among losses can be written as

$$\begin{aligned} T_h &= 3 \\ T_0 (1 - L_w) + T_h L_w &= 84 \\ T_0 (1 - L_w L_c) + T_h L_w L_c &= 117 \\ T_0 (1 - L_t) + T_p L_t &= 130, \end{aligned} \quad (1)$$

where,  $T_h$  and  $T_p$  are the equivalent temperatures of the horn and the paraboloid, respectively, when they are directed toward the zenith;  $T_0$  is the atmospheric temperature of 303°K;  $L_w$ ,  $L_c$  and  $L_t$  are coefficients of losses in the waveguide feeder, coaxial cable and the total transmission lines, respectively. Since  $L_t$  contains the loss of a curved waveguide on the aerial mount 0.07 times as long as the main waveguide feeder of about 24 metre, it may be written

$$L_t = L_w^{1.07} L_c. \quad (2)$$

Solving these equations, we obtained

$$\begin{aligned} L_w &= 0.73 \quad (1.37 \text{ db}) \\ L_c &= 0.85 \quad (0.70 \text{ db}) \\ L_t &= 0.61 \quad (2.16 \text{ db}) \\ T_p &= 18. \end{aligned} \quad (3)$$

It is to be mentioned here that the gain of the unit aerial was 1920 according to the measurement at this time, a gain a little less than that reported in the last Proceedings<sup>1)</sup>.

#### IV. Quarter-wavelength plates

There are several ways available to receive circularly polarized waves at microwave frequencies. Typical methods are (1) to place an array of metal strips in front of the aerial, (2) to use a circular waveguide containing a phase shifter and (3) to use a turnstile junction. With a single aerial, (2) or (3) is perhaps most convenient but we chose (1) because of its simplicity and reliability.

##### 1. Design

The design of an array consisting of an infinite number of semi-infinite metallic

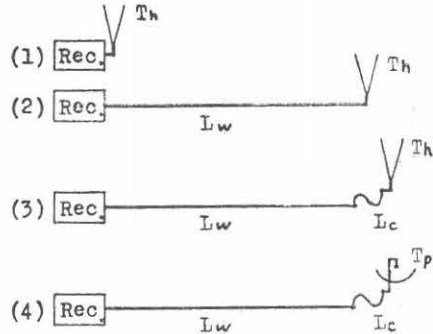


Fig. 2. The process of transmission-loss measurement.

obstacles of zero thickness with edges parallel to the electric field is given in the reference 3. The data may be available also for our purpose if higher modes produced at one end of the grating will sufficiently attenuate at the other. In addition, the reflection may be cancelled in this case if the effective path-length in the grating is an integral number of a half wavelength because both sides of the grating have the same impedance. Referring to Fig. 3,

$$l_1/\lambda - l_2/\lambda_g = 1/4 \quad (4)$$

$$l_2/\lambda_g = n/2 \quad (n \text{ is a positive integer}) \quad (5)$$

$$\lambda_g = \lambda/\sqrt{1 - (\lambda/2a)^2} \quad (6)$$

From equations (4) and (5),  $l_1$  can be written

$$l_1 = (2n+1)\lambda/4, \quad (7)$$

and from Fig. 4,

$$l_2 = l_1 + 2(d' - d) = (2n+1)\lambda/4 + 2\alpha a/\pi, \quad (8)$$

$$\text{where, } \alpha = z/a \quad (d' - d). \quad (9)$$

Thus from equations (5), (6) and (8),

$$\lambda^2 = \{1 - (\lambda/2a)^2\} \{ (2n+1)\lambda/2n + 4\alpha a/n\pi \}^2. \quad (10)$$

Spacing "a" for a certain n can be determined from equation (10) if  $\alpha$  is assumed. But we must repeat calculations several times until the result is consistent with the data in the reference. From "a" thus obtained,  $l_1$  and d can be determined and so the actual length l is

$$l = l_1 - 2d \quad (11)$$

The results of calculations are shown in Table 1. The value n cannot exceed 3 because the second higher mode comes within the cutoff.

Table 1. Design data for the quarter-wavelength plate

n	units are "mm"				attenuation of $H_{02}$ wave through l in db	power reflection at each end in percent	at $\pm 100$ Mc/s	
	a	l	d	d' - d			transmitting power reversal/normal in percent	power reflection in percent
1	49.3	45.4	5.4	0.8	38	4.5	0.10	0.59
2	60.4	79.3	7.2	1.0	43	1.5	0.08	0.38
3	68.6	112.7	9.3	1.6	36	0.8	0.19	0.54

In Table 1, attenuation of  $H_{02}$  mode through l is calculated from

$$54.57\sqrt{1 - (a/\lambda)^2}/a \quad \text{db/m}^{(1)}, \quad (12)$$

and the power reflection at each end of the grating is

$$(1 - Y^2)/(1 + Y^2)^2, \quad (13)$$

where,  $Y = \lambda/\lambda_g$ . (14)

The resultant power reflection can be calculated referring to the equivalent circuit in Fig. 3, where the line  $l_2$  having impedance Y is inserted between the lines of impedance 1, that is,

$$(1 - Y^2)^2 / \{4Y^2 \cot^2(2\pi l_2/\lambda_g) + (1 + Y^2)^2\}. \quad (15)$$

Equation (15) shows that, under the worst conditions, the reflection is,

$(1 - Y^2)^2 / (1 + Y^2)^2$ , which is more than 10 percent if  $Y < 0.72$ .

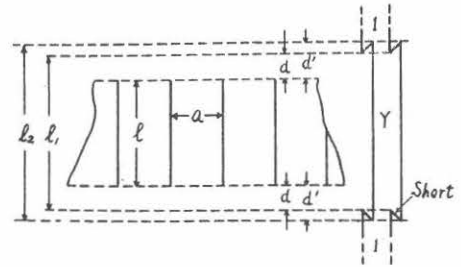


Fig. 3. A quarter-wavelength plate and the equivalent circuit.

At a frequency far apart from that used for the design, the phase of the electric field parallel to the strips generally leads that of the perpendicular field by  $\pi/2 + \Delta\phi$ . In these circumstances, the transmitting power ratio of the inversely polarized wave to the normal wave of equal intensity is  $\tan^2 (\pi/4 - \Delta\phi/2)$ .

It may be concluded from Table 1 that  $n=2$  is most satisfactory on account of its large attenuation against higher modes and its good frequency response.

## 2. Structure

A quarter-wavelength plate has a round frame, 155 cm in diameter, in which 23 strips, each 1 mm thick and 79 mm wide, are arranged with equal spacings of 61 mm. Eight of these plates are mounted over the eight paraboloids 40 cm apart from the edges. These plates can be driven by a common shaft having a crank. Nine revolutions of the shaft result in 90 degrees rotation of the gratings. It takes us a few seconds to complete one process.

## 3. Tests

The following experiments show that the design is satisfactory for practical use.

**Reflection:** No change could be observed on the record when a grating was rotated slowly over 360 degrees after the input of the aerial under test was separately led to the receiver. The result was the same whether the aerial was directed toward the sun or towards the empty sky.

**Phase relations:** The correct phase relations adjusted before we mount the gratings were kept unchanged after gratings were placed in position. This proves that all gratings are practically uniform.

**Sensitivity to the inversely polarized wave:** Undesirable sensitivity to the inversely polarized wave was measured by an indirect method. When a resultant signal from a pair of neighboring aerials are led to the receiver as in Fig. 4 (a), an almost sinusoidal record is obtained. But when the gratings are normal to each other as in Fig. 4 (b), the record should be kept unchanged because both components of a randomly polarized wave have no correlation with each other. The result of experiments was consistent with the theory, which proves that the aerial system is practically insensitive to the inversely polarized component.

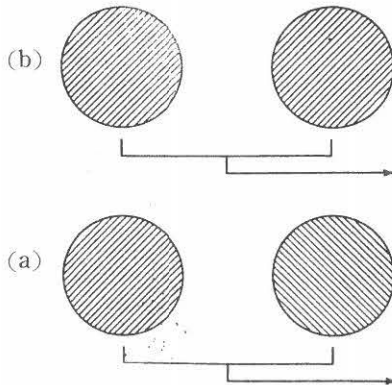


Fig. 4. Measurement of sensitivity to the inversely polarized wave.

## 1. Square-law detector

As a matter of course, the use of a square-law detector is desirable for noise measurements. In addition, the output fluctuation is almost the same in either case where a square-law detector or a linear detector is used. Therefore we introduced a square-law detector of vacuum tube type into the receiver. The supply voltage of the

## V. Improvement of the radiometer

Although most parts of the radiometer are the same as those described in detail in the last Proceedings, some alterations have been made to improve the accuracy of measurement.

detector tube must be stabilized as much as possible, because the detector is, in turn, the first stage of a high gain low-frequency amplifier. It must be noted here that the gain variation of the amplifier before the detector exerts twice as much influence on the whole stability as the case when using a linear detector, so that the intermediate-frequency amplifier must be stabilized to a higher degree. The improved stabilized sources developed here are shown in Figs. 5 and 6.

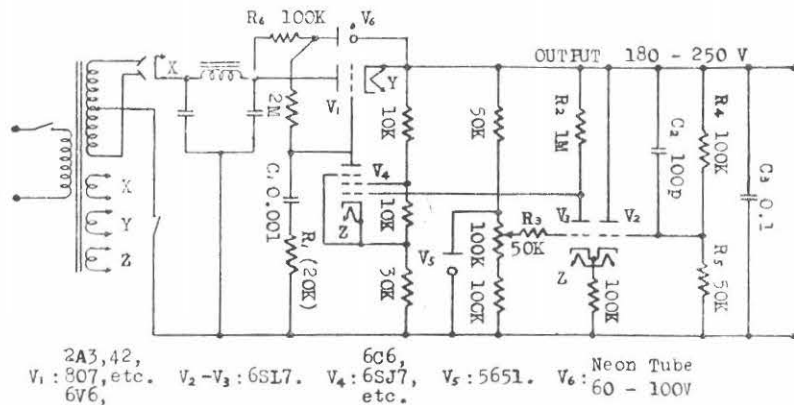


Fig. 5. D.C. voltage regulator.

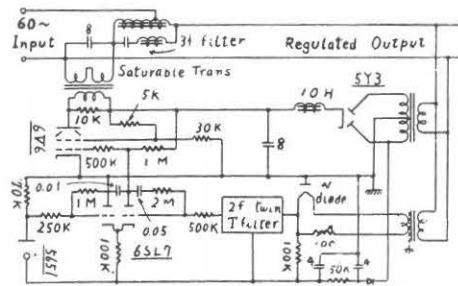


Fig. 6. A.C. voltage regulator.

## 2. Daily calibrations by a hot load

The so called sky temperature<sup>5)</sup> may be available as a standard noise level of a radiometer if an aerial is placed close to the receiver. However, when the transmission loss is large as in the present case, the input noise changes with the atmospheric temperature even though aeriels are pointed to the zenith. Therefore we have prepared a hot load<sup>2)</sup> for daily calibrations of the radiometer. As we have already pointed out in section II, a feeder of a considerable length is inserted between the switch and the receiver for reducing errors due to the "substitution".<sup>2)</sup> The level of the "sky temperature" is also recorded every day to watch the attenuation of the transmission lines. The maximum attenuation ever recorded in the rainy season was five percent larger than that in the dry season.

## 3. Linear recording

As the square-law detector is used, D.C. output voltage of the synchronous rectifier is linearly related with the input power of the receiver. Therefore a linear D.

C. voltage-current transformer is desirable to facilitate calibrations. The network used is shown in Fig. 7. It is rather complicated because the rectangular co-ordinate type recorder requires somewhat larger driving power. The recorder is connected between two voltage regulators of the same connections as shown in Fig. 5, and the signal is applied in series to one of the reference terminals of each regulator. Excellent stability, linearity and quick response have been obtained on account of the high loop gain of each regulator.

#### IV. Observational techniques

Somewhat different ways have been employed since the 8-element interferometer was completed.

##### 1. Adjustment of phase relations

As the first step, we direct No. 1 and No. 2 aerials toward the sun and the others towards the zenith. Magic-tee switches are then properly adjusted to avoid the loss of signal. After the sun is scanned two or three times, we direct No. 3 aerial toward the sun and No. 1 toward the zenith, and so on. When finished scanning by No. 7 and No. 8 aerials, we retrace the same course from the beginning. After these processes are repeated two or three times, we compare the phase of each sinusoidal record thus obtained with the theoretical record. We correct the length of the waveguide at each 0.5 mm step, referring to the above data and repeat experiments until phase errors decrease to within  $\pm 2$  degrees. We make it a rule to examine the phase relations every six months.

##### 2. Daily observations

After the preliminary operation of the radiometer for one or two hours, we set the recorder pen at the position corresponding to the atmospheric temperature; the input of the 1-f amplifier is then short-circuited. Opening the circuit, we introduce the output of the hot load into the receiver and adjust the gain of the 1-f amplifier so that the recorder pen indicates 573°K which is equal to the temperature of the hot load. Then we record the "sky temperature" and finally we put the interferometer into full operation. Calibration of the equipment is made also at the end of the observation.

While the sun is quiet, observation is made for about half an hour during which five drift curves are recorded for each polarization. But when the sun is active, fifty drift curves are taken on each side of the local noon to locate the radio spots on the solar disk in two dimensional sense.

To our regret, this method is not available for the periods around the equinoxes.

#### VII. Acknowledgement

The authors wish to express their deep gratitude to Prof. A. Kimpara, director of our Institute, Prof. Y. Hagihara and other members of the Japanese National

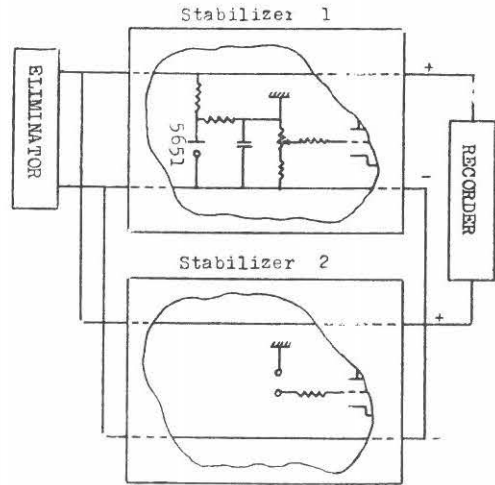


Fig. 7. A sketch of a linear D.C. voltage-current transformer.

Committee of U. R. S. I. for their unceasing encouragement in our studies. They also wish to acknowledge Messrs. H. Jindo, T. Takayanagi and C. Torii, members of the Radio Astronomy Section, for their enthusiastic assistance in constructing the interferometer.

### References

- 1) H. Tanaka and T. Kakinuma: Proc. Res. Inst. Atm., II, p. 53 (1954).
- 2) H. Tanaka and T. Kakinuma: Proc. Res. Inst. Atm., II, p. 77 (1954).
- 3) M.I.T. Rad. Lab. Ser.: Waveguide Handbook, p. 290 (1951).
- 4) M.I.T. Rad. Lab. Ser.: Waveguide Handbook, p. 28 (1951).
- 5) H. Tanaka and T. Kakinuma: Proc. Res. Inst. Atm., I, p. 85 (1953).